Damage-enhanced order reduction models for 2D woven composites based on data-driven multiscale mechanics

Tianyu ZHANG[1]

joint work with Ling WU[1], Ludovic NOELS[1]

[1]Computational & Multiscale Mechanics of Materials (LTAS-CM3)
Aerospace and Mechanical Engineering Department
University of Liège, Belgium

CSMA, 16-20 May, 2022, Giens, France

Context

2D woven composites

- periodic heterogeneous multiscale materials that can be described by RVEs
  - mesoscale ($\sim 10^{-3}$ m) RVE: matrix + warp and weft yarns
  - microscale ($\sim 10^{-6}$ m) RVE of yarns: UD fibres + matrix
- damage-enhanced nonlinear behaviours for constituents
  - fibres: transversely isotropic linear elasticity
  - matrix: isotropic J_2 elasto-plasticity
- numerical modelling and simulation
  - complex geometrical description and material properties assignment
  - high computational cost (time and memory usage)

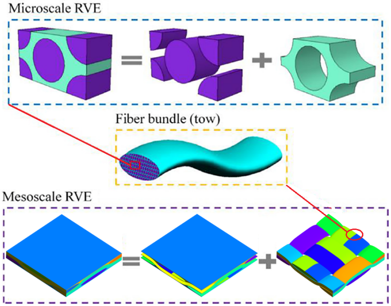

Figure: Multiscale description of a 2D woven composite [Wang et al. 2017]

Context

Mean-Field Homogenisation (MFH) for yarns

- semi-analytical solution for the extended Eshelby problem with multiple inclusions

$$\bar{\varepsilon} = v_{\mathsf{I}}\varepsilon_{\mathsf{I}} + v_0\varepsilon_0\,, \quad \bar{\boldsymbol{\sigma}} = v_{\mathsf{I}}\boldsymbol{\sigma}_{\mathsf{I}} + v_0\boldsymbol{\sigma}_0$$

- Linear Comparison Composite (LCC)-based nonlinear framework

$$\Delta\varepsilon_{\mathsf{I}} = \mathbb{B}^{\epsilon}\left(\mathsf{I},\, \mathbb{C}_{\mathsf{I}}^{\mathsf{LCC}},\, \mathbb{C}_0^{\mathsf{LCC}}\right) : \Delta\varepsilon_0$$

- Mori-Tanaka (MT) model

$$\mathbb{B}^{\epsilon}\left(\mathsf{I},\, \mathbb{C}_{\mathsf{I}}^{\mathsf{LCC}},\, \mathbb{C}_0^{\mathsf{LCC}}\right) = \left\{\mathbb{I} + \mathbb{S}\left(\mathsf{I},\, \mathbb{C}_0^{\mathsf{LCC}}\right) : \left[\left(\mathbb{C}_0^{\mathsf{LCC}}\right)^{-1} : \mathbb{C}_{\mathsf{I}}^{\mathsf{LCC}} - \mathbb{I}\right]\right\}^{-1}$$

Context

Full-order FE modelling and damage-enhanced MFH-based nonlinear Direct Numerical Simulation (DNS) ([Wu, Maillard, and Noels 2021] and [Wu et al. 2021])

- computational cost: 63189 elements; ~ 3 days
- still too high for applications of industrial complexity

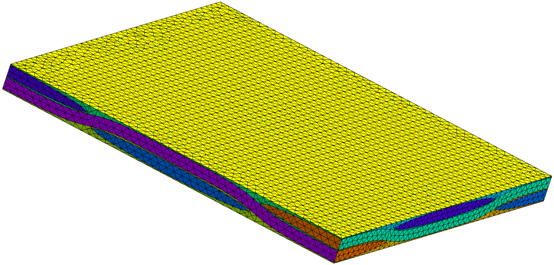

Figure: FE model of a 2D woven RVE at mesoscale

Problematic

Propose a reduced-order model (ROM) for 2D woven composites by embedding

- micromechanics-based homogenization methods
- data-driven model reduction techniques

to conduct accurately and efficiently damaged-enhanced nonlinear multiscale analysis

Outline

Outline

Deep Material Network (DMN)

Deep Material Network (DMN) [Liu and Wu 2019]: a ROM for RVE

- mechanistic building blocks-based tree structure: homogenization + rotation
- efficient offline training in linear elastic regime: geometrical parameters fitting
- accurate online extrapolation in arbitrary unknown nonlinear inelastic regime: mechanical response prediction

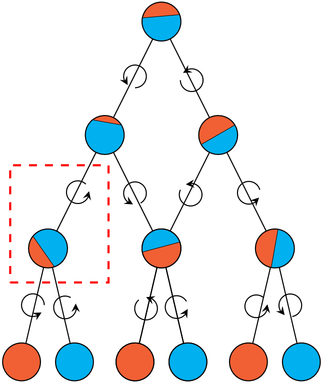

Figure: Illustration of a 3-layer DMN for a biphasic material

VM scheme

DMN-liked VM scheme [Wu, Adam, and Noels 2021]: 2D woven RVE ≈ Short Fibre Reinforced Matrix (SFRM) pseudo-grains aggregate

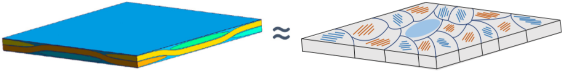

- step 1: matrix + fibres ⇒ MFH ⇒ SFRM
- step 2: SFRMs ⇒ Voigt's rule of mixtures ⇒ 2D woven RVE
- parameters: $\boldsymbol{\chi}^{\mathrm{VM}} = \left\{ v_i,\, \boldsymbol{\theta}_i,\, \alpha_i \mid i = 1, ..., N_{\mathrm{s}};\ \sum_{i=1}^{N_{\mathrm{s}}} v_i = 1.0 - v_0 \right\}$

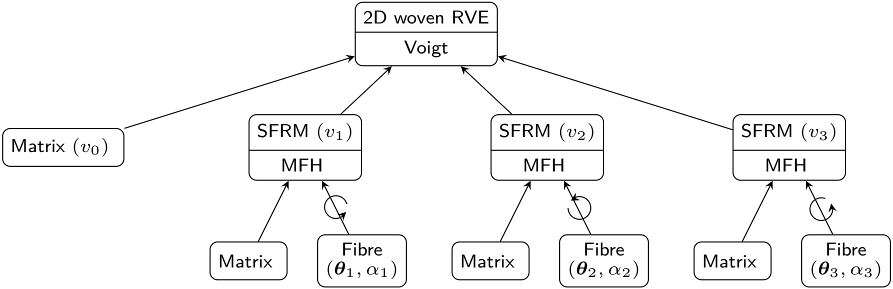

Figure: Illustration of the VM scheme ($N_{\mathrm{s}} = 3$)

LVM scheme

DMN-liked LVM scheme [Wu, Adam, and Noels 2021]: 2D woven RVE ≈ 2-ply laminate

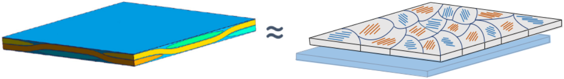

- step 1: matrix + fibres ⇒ MFH ⇒ SFRM
- step 2: SFRMs ⇒ Voigt's rule of mixtures ⇒ SFRMs aggregate
- step 3: matrix ply + aggregate ply ⇒ Laminate theory ⇒ 2D woven RVE
- parameters: $\boldsymbol{\chi}^{\text{LVM}} = \left\{ v_i, \boldsymbol{\theta}_i, \alpha_i \mid i = 1, ..., N_\text{s}; \sum_{i=1}^{N_\text{s}} v_i = 1.0 \right\}$

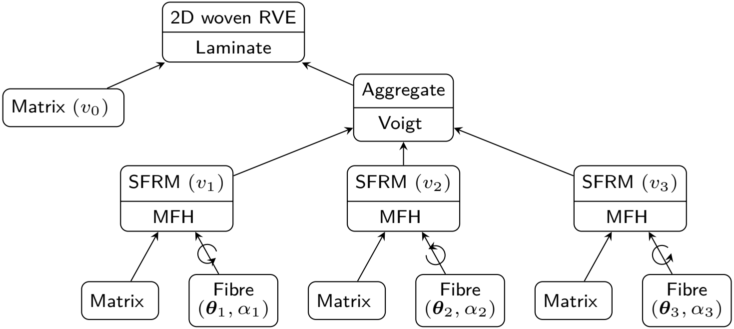

Figure: Illustration of the LVM scheme $(N_\text{s} = 3)$

VLM scheme

DMN-liked VLM scheme [Wu, Adam, and Noels 2021]: 2D woven RVE ≈ 2-ply laminate pseudo-grains aggregate

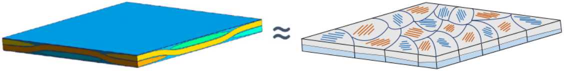

- step 1: matrix + fibres ⇒ MFH ⇒ SFRM
- step 2: matrix ply + SFRM ply ⇒ Laminate theory ⇒ 2-ply laminate
- step 3: 2-ply laminate aggregate ⇒ Voigt's rule of mixtures ⇒ 2D woven RVE
- parameters: $\chi^{\text{VLM}} = \left\{ v_i^{\text{g}},\ \boldsymbol{\theta}_i^{\text{g}},\ v_i^{\text{m}},\ \boldsymbol{\theta}_i^{\text{f}},\ \alpha_i \mid i = 1, \ldots, N_{\text{s}};\ \sum_{i=1}^{N_{\text{s}}} v_i^{\text{g}} = 1.0;\ \sum_{i=1}^{N_{\text{s}}} v_i^{\text{g}} v_i^{\text{m}} = v_0 \right\}$

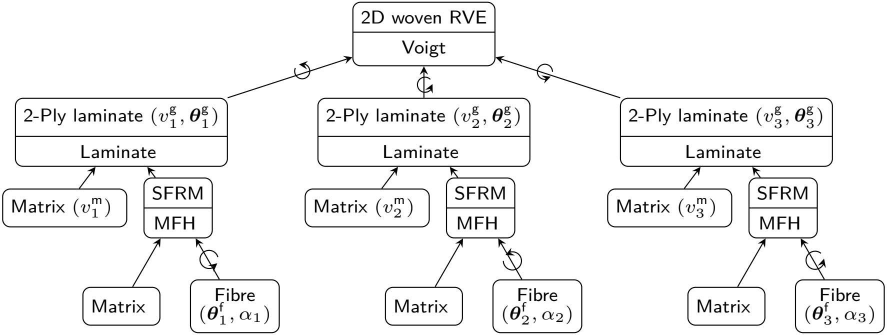

Figure: Illustration of the VLM scheme $(N_{\text{s}} = 3)$

Outline

Offline training

Identification of χ^{opt} in linear elasticity by solving

$$\chi^{\text{opt}} = \arg\min_{\chi} L(\hat{\mathbb{C}}(\gamma),\, \bar{\mathbb{C}}(\chi|\gamma_s))$$

with

- $\hat{\mathbb{C}}(\gamma)$: homogenized elasticity tensor given by computational homogenization on a full-order model parametrized by $\gamma = \left(E_0, \nu_0, E_{\mathsf{I}}^{\mathsf{T}}, E_{\mathsf{I}}^{\mathsf{L}}, \nu_{\mathsf{I}}^{\mathsf{LT}}, \nu_{\mathsf{I}}^{\mathsf{TT}}, G_{\mathsf{I}}^{\mathsf{LT}}\right)$
- $\bar{\mathbb{C}}(\chi|\gamma_s)$: homogenized elasticity tensor given by VM, LVM or VLM scheme parametrized by χ^{VM}, χ^{LVM} or χ^{VLM} for given γ
- loss function: ($G(\chi)$ is a volume fraction consistency function)

$$L(\hat{\mathbb{C}},\, \bar{\mathbb{C}}(\chi)) = \frac{1}{n}\sum_{s=1}^{n} \frac{\|\hat{\mathbb{C}}(\gamma_s) - \bar{\mathbb{C}}(\chi|\gamma_s)\|}{\|\hat{\mathbb{C}}(\gamma_s)\|} + \frac{\lambda}{2} G(\chi)$$

Online evaluation

Extrapolation to unknown material and loading spaces: NR iterative resolution for nonlinear equations

- top-bottom backward de-homogenisation process
- bottom-top forward homogenisation process

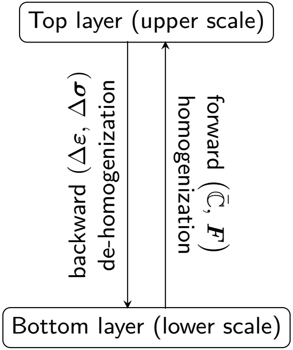

Outline

Uniaxial (cyclic) tensile test & In-plane cyclic shear test

- training results is available in [Wu, Adam, and Noels 2021]
- damage-free nonlinear predictions with
  - fibres: transversely isotropic linear elasticity
  - matrix: isotropic J_2 elasto-plasticity

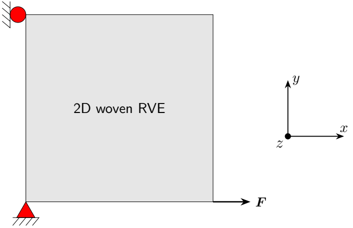

Figure: Uniaxial tensile test

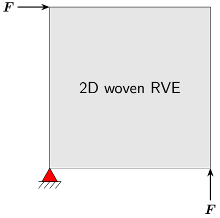

Figure: In-plane shear test

- comparison of the CPU time

	Tensile	Shear
DNS	11 h	76 h
VM	30 s	22 s
LVM	35 s	25 s
VLM	35 s	22 s

Uniaxial (cyclic) tensile test & In-plane cyclic shear test

- comparison of the global responses for the uniaxial tensile (cyclic) test

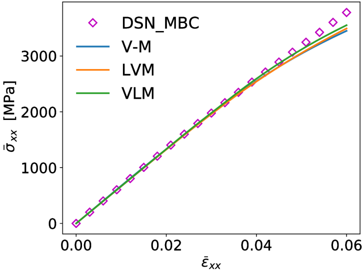

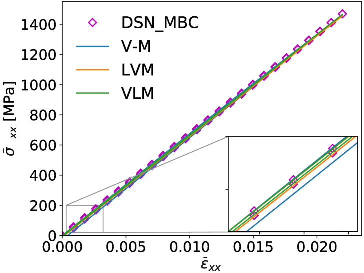

- comparison of the global responses for the in-plane cyclic shear test

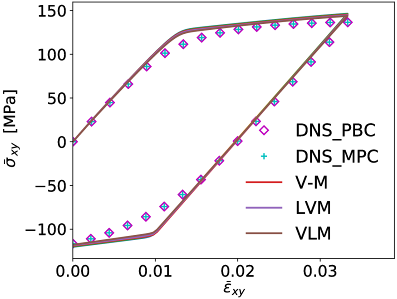

Local damage models calibration

Non-local damage models are used for DNS

- phase field-liked damage model for fibres, Lemaitre-like damage model for matrix [Wu et al. 2021]

Local damage models are used for VM, LVM and VLM

- no physical "characteristic length" between material nodes
- Weibull-like damage model for fibres, Lemaitre-like damage model for matrix [Wu, Maillard, and Noels 2021]

Calibration with an uniaxial tensile test on a UD composite sample

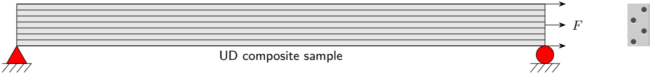

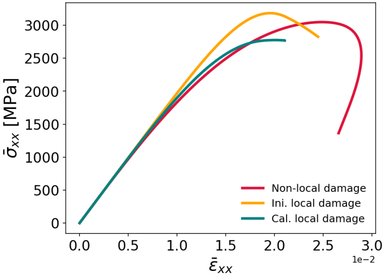

Damage-enhanced uniaxial tensile test - Load until failure

Comparison of the global responses

	Strength [GPa]
DNS	891.778
VM	892.981
rel. err. (%)	0.13
LVM	852.096
rel. err. (%)	4.45
VLM	913.868
rel. err. (%)	2.48

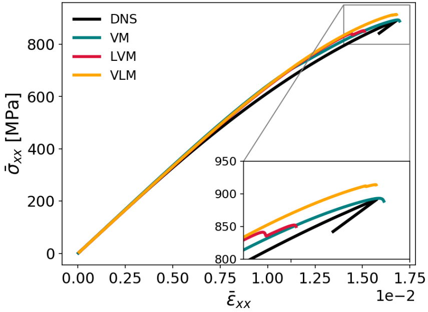

Uniaxial tensile test - Load until failure

LVM training results and responses of the two plies

- Aggregate ply takes the majority load
- Grains 9, 10, 19 and 20 have a small α

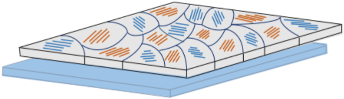

Grain	α
1 (weft) & 2 (warp)	216.645
3 (weft) & 4 (warp)	258.721
5 (weft) & 6 (warp)	195.969
7 (weft) & 8 (warp)	181.194
9 (weft) & 10 (warp)	21.032
11 (weft) & 12 (warp)	247.153
13 (weft) & 14 (warp)	204.540
15 (weft) & 16 (warp)	123.377
17 (weft) & 18 (warp)	298.981
19 (weft) & 20 (warp)	23.852

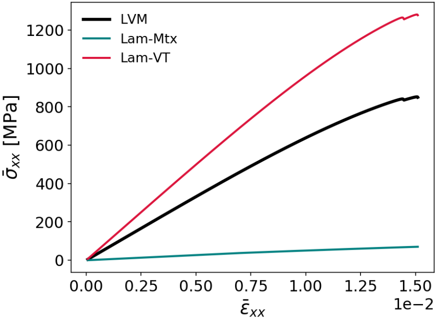

Uniaxial tensile test - Load until failure

Matrix and fibres damage evolution in the grains of the aggregate ply:

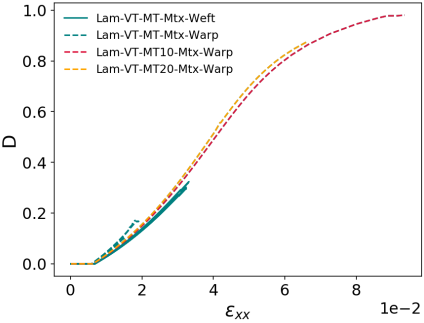

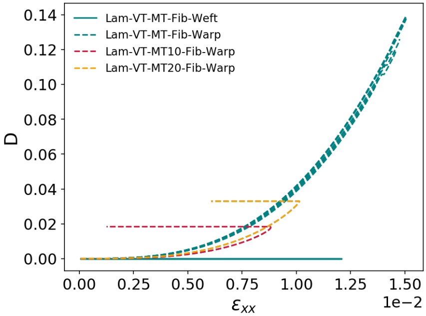

Uniaxial tensile test - Load until failure

- Deactivation of matrix damage in
  - VM: grains 2 and 3
  - LVM: grains 9, 10, 19 and 20

- Comparison of the global responses:

	Strength [GPa]	CPU Time
DNS	891.778	64 h
VM	892.981	19 s
rel. err. (%)	0.13	
VM-Mod.	931.430	
rel. err. (%)	4.45	
LVM	852.096	6 mins
rel. err. (%)	4.45	
LVM-Mod.	918.646	
rel. err. (%)	3.01	
VLM	913.868	17 mins
rel. err. (%)	2.48	

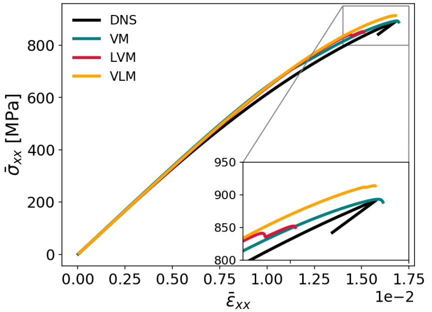

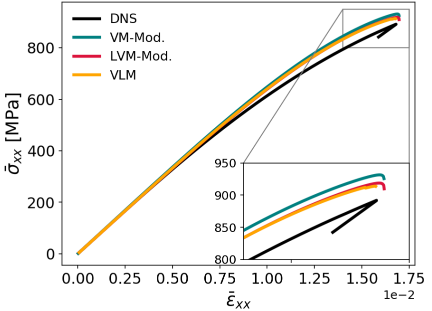

Uniaxial tensile test - Load until failure

Comparison of matrix damage state

- DNS

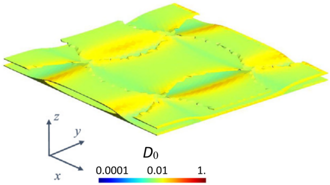

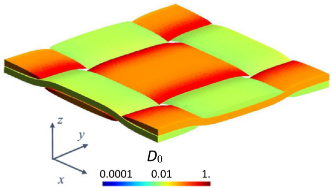

- VM

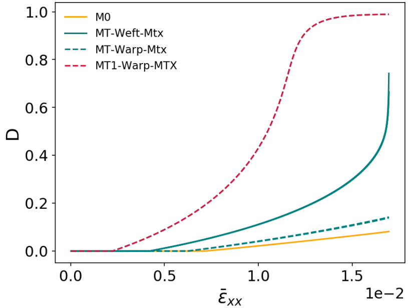

Uniaxial tensile test - Load until failure

Comparison of fibres damage state (DNS vs. VM)

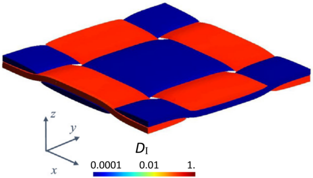

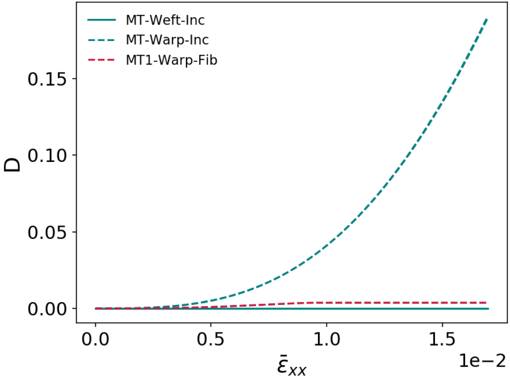

Outline

Conclusions and outlooks

Conclusions

- Construction of DMN-liked and micromechanics-based damage-enhanced ROMs (VM, LVM and VLM) for 2D woven composites
- Efficient offline learning only in linear elasticity
- Accurate online extrapolation to arbitrary unknown nonlinear inelastic material laws and loading spaces

Outlooks

- Improvement of the accuracy by considering more suitable damage models
- Application for 3D woven composites and for other types of composites

Thanks for your attention !

References I

Liu, Z. and C. Wu (2019). "Exploring the 3D architectures of deep material network in data-driven multiscale mechanics". In: *Journal of the Mechanics and Physics of Solids* 127, pp. 20–46.

Sun, Z. et al. (2020). "Numerical analysis of out-of-plane thermal conductivity of C/C composites by flexible oriented 3D weaving process considering voids and fiber volume fractions". In: *Journal of Materials Research* 35.14, pp. 1888–1897.

Wang, L. et al. (2017). "Progressive failure analysis of 2D woven composites at the meso-micro scale". In: *Composite structures* 178, pp. 395–405.

Wu, L., L. Adam, and L. Noels (2021). "Micro-mechanics and data-driven based reduced order models for multi-scale analyses of woven composites". In: *Composite Structures* 270, p. 114058.

Wu, L., E. Maillard, and L. Noels (2021). "Tensile failure model of carbon fibre in unidirectionally reinforced epoxy composites with mean-field homogenisation". In: *Composite Structures* 273, p. 114270.

Wu, L. et al. (2021). "Per-phase spatial correlated damage models of UD fibre reinforced composites using mean-field homogenisation; applications to notched laminate failure and yarn failure of plain woven composites". In: *Computers & Structures* 257, p. 106650.

Local damage evolution (VM, LVM or VLM)

$$D_{\mathsf{l}} = \varphi + \varrho \sqrt{\frac{\varphi(1-\varphi)}{N}}$$

with

- $\varphi(\hat{\sigma}_{\mathsf{l}}^{\mathsf{zz}}) \sim$ Weibull distribution, with $\hat{\boldsymbol{\sigma}}_{\mathsf{l}} = \mathbb{C}_{\mathsf{l}}^{\mathsf{el}} : \boldsymbol{\varepsilon}_{\mathsf{l}}$
- ϱ one realisation of $P \sim \mathcal{N}(0, 1)$, and N the number of fibres in a bundle

Non-local damage evolution (full-order model)

$$D_{\mathsf{l}}(x,\, t) = 1 - (1 - d_{\mathsf{l}}(x,\, t))^n$$

with

- $d_{\mathsf{l}}(x,\, t)$ given by the phase-field model
- $n \in [2,\, 3]$ shape parameter

Local (VM, LVM or VLM) and non-local (full-order model) damage evolution

$$D_0 = \frac{D_0^{\mathsf{max}}}{1 - \frac{1}{1+\exp\left\{\left(s_0 p_{\mathsf{C}_0}\right)\right\}}} \left(\frac{1}{1+\exp\{(-s_0(\chi_0 - p_{\mathsf{C}_0}))\}} - \frac{1}{1+\exp\{(s_0 p_{\mathsf{C}_0})\}} \right)$$

with

- D_0^{max} the saturation damage level
- s_0 and p_{C_0} two material parameters
- $\chi_0(t)$ guarantee of the irreversibility
  - local: $\chi_0(t) = \max_{\tau \in [0,\, t]} (p_0)$ with $\dot{p}_0 = \sqrt{\frac{2}{3} \dot{\boldsymbol{\varepsilon}}_0^{\mathsf{pl}} : \dot{\boldsymbol{\varepsilon}}_0^{\mathsf{pl}}}$
  - non-local: $\chi_0(\boldsymbol{x},\, t) = \max_{\tau \in [0,\, t]} (\tilde{p}_0)$ with $\tilde{p}_0 - \nabla \cdot (\boldsymbol{c}_0 \cdot \nabla \tilde{p}_0) = p_0$

Information paths for a parent node with N_d direct child nodes

- top-bottom strain distribution:

$$\Delta\varepsilon = \begin{cases} \sum_{i=1}^{N_\mathsf{d}} v_i^\mathsf{d} \Delta\varepsilon_i^\mathsf{d}, & \text{for MFH-based and 2-ply laminate-based node} \\ \{\Delta\varepsilon_i^\mathsf{d}\}_{i=1,\ldots,N_\mathsf{d}}, & \text{for Voigt's mixtures-based node} \end{cases}$$

- bottom-top stress and algorithmic operator collection:

$$\boldsymbol{\sigma} = \sum_{i=1}^{N_\mathsf{d}} v_i^\mathsf{d} \boldsymbol{\sigma}_i^\mathsf{d}$$

$$\mathbb{C}^{\mathsf{alg}} = \mathbb{C}^{\varepsilon\varepsilon} = \frac{\mathsf{d}\boldsymbol{\sigma}}{\mathsf{d}\varepsilon} = \sum_{n=1}^{N_\mathsf{d}} v_n^\mathsf{d} \mathbb{C}_n^{\mathsf{alg,\ d}} : \frac{\mathsf{d}\varepsilon_n^\mathsf{d}}{\mathsf{d}\varepsilon}$$

Linearisation of the composite parent node by a damage-enhanced incremental-secant-based Linear Comparison Composite (LCC)

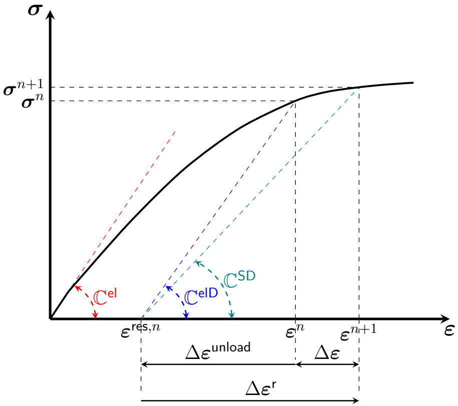

Figure: Composite parent node linearisation

- unloading: (i for fibre and matrix)

$$\boldsymbol{\varepsilon}^{n}, \boldsymbol{\sigma}^{n}, D_i^{n}$$

$$\downarrow$$

$$\text{LCC} \quad \mathbb{C}^{\mathsf{elD}}(v_i, \mathbb{C}_i^{\mathsf{elD}}, \mathsf{I})$$

$$\downarrow$$

$$\boldsymbol{\varepsilon}^{\mathsf{res},n} = \boldsymbol{\varepsilon}^{n} - \Delta\boldsymbol{\varepsilon}^{\mathsf{unload}}$$
$$\boldsymbol{\sigma}^{\mathsf{res},n} = 0$$

- reloading: (i for fibre and matrix)

$$\Delta\boldsymbol{\varepsilon}^{\mathsf{r}}, D_i^{n+1}$$

$$\downarrow$$

$$\text{LCC} \quad \mathbb{C}^{\mathsf{SD}}(v_i, \mathbb{C}_i^{\mathsf{SD}}, \mathsf{I})$$

$$\downarrow$$

$$\boldsymbol{\varepsilon}^{n+1} = \boldsymbol{\varepsilon}^{\mathsf{res},n} + \Delta\boldsymbol{\varepsilon}^{\mathsf{r}}$$
$$\boldsymbol{\sigma}^{n+1} = \mathbb{C}^{\mathsf{SD}} : \Delta\boldsymbol{\varepsilon}^{\mathsf{r}}$$

Appendix B.1 - Nonlinear analysis for MFH-based node

Linearisation of the fibre child node by a damage-enhanced transversely isotropic elastic material with $E_{\mathrm{I}}^{\mathrm{zD}} = (1 - D_{\mathrm{I}})E_{\mathrm{I}}^{\mathrm{z}}$ and $\nu_{\mathrm{I}}^{\mathrm{zxD}} = (1 - D_{\mathrm{I}})\nu_{\mathrm{I}}^{\mathrm{zx}}$

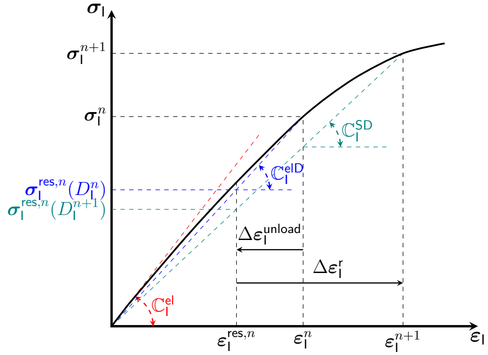

Figure: Fibre child node linearisation

- unloading:

$$\boxed{\boldsymbol{\varepsilon}_{\mathrm{I}}^{n},\, \boldsymbol{\sigma}_{\mathrm{I}}^{n},\, D_{\mathrm{I}}^{n}}$$

$$\downarrow$$

$$\boxed{\text{Fibre} \mid \mathbb{C}_{\mathrm{I}}^{\mathrm{elD}}(E_{\mathrm{I}}^{z\mathrm{D}}, E_{\mathrm{I}}^{x}, \nu_{\mathrm{I}}^{\mathrm{zxD}}, \nu_{\mathrm{I}}^{\mathrm{xy}}, \mu_{\mathrm{I}}^{\mathrm{zx}})}$$

$$\downarrow$$

$$\boxed{\begin{aligned} \boldsymbol{\varepsilon}_{\mathrm{I}}^{\mathrm{res},\,n} &= \boldsymbol{\varepsilon}_{\mathrm{I}}^{n} - \Delta\boldsymbol{\varepsilon}_{\mathrm{I}}^{\mathrm{unload}} \\ \boldsymbol{\sigma}_{\mathrm{I}}^{\mathrm{res},\,n} &= \mathbb{C}_{\mathrm{I}}^{\mathrm{elD}}(D_{\mathrm{I}}^{n}) : \boldsymbol{\varepsilon}_{\mathrm{I}}^{\mathrm{res},\,n} \end{aligned}}$$

- reloading:

$$\boxed{\Delta\boldsymbol{\varepsilon}_{\mathrm{I}}^{\mathrm{r}},\, D_{\mathrm{I}}^{n+1}}$$

$$\downarrow$$

$$\boxed{\text{Fibre} \mid \mathbb{C}_{\mathrm{I}}^{\mathrm{SD}} = \mathbb{C}_{\mathrm{I}}^{\mathrm{elD}}}$$

$$\downarrow$$

$$\boxed{\begin{aligned} \boldsymbol{\varepsilon}_{\mathrm{I}}^{n+1} &= \boldsymbol{\varepsilon}_{\mathrm{I}}^{\mathrm{res},\,n} + \Delta\boldsymbol{\varepsilon}_{\mathrm{I}}^{\mathrm{r}} \\ \boldsymbol{\sigma}_{\mathrm{I}}^{n+1} &= \boldsymbol{\sigma}_{\mathrm{I}}^{\mathrm{res},\,n} + \mathbb{C}_{\mathrm{I}}^{\mathrm{SD}}(D_{\mathrm{I}}^{n+1}) : \Delta\boldsymbol{\varepsilon}_{\mathrm{I}}^{\mathrm{r}} \end{aligned}}$$

Appendix B.1 - Nonlinear analysis for MFH-based node

Linearisation of the matrix child node by a damage-enhanced isotropic J_2 elasto-plastic material with $\kappa_0^{\mathsf{D}} = (1 - D_0^n)\kappa_0$, $\mu_0^{\mathsf{D}} = (1 - D_0^n)\mu_0$ and $\mu_0^{\mathsf{SD}} = (1 - D_0^n)\mu_0^{\mathsf{S}} = (1 - D_0^n)\left(\mu_0 - (3\mu_0^2\dot{p})/(\mathbb{C}_0^{\mathsf{el}} : \Delta\boldsymbol{\varepsilon}_0^{\mathsf{r}})^{\mathsf{eq}}\right)$

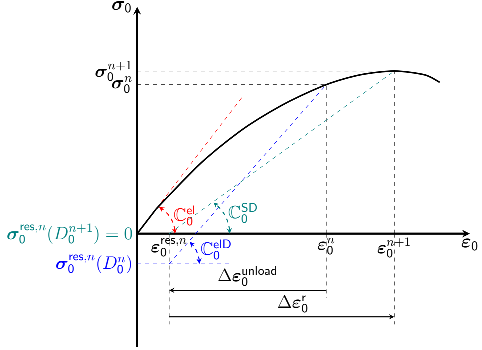

Figure: Matrix child node linearisation

- unloading:

$\boldsymbol{\varepsilon}_0^n$, $\boldsymbol{\sigma}_0^n$, D_0^n

$\downarrow$

Matrix	$\mathbb{C}_0^{\mathsf{elD}}(\kappa_0^{\mathsf{D}}, \mu_0^{\mathsf{D}})$

$\downarrow$

$$\boldsymbol{\varepsilon}_0^{\mathsf{res},n} = \boldsymbol{\varepsilon}_0^n - \Delta\boldsymbol{\varepsilon}_0^{\mathsf{unload}}$$
$$\boldsymbol{\sigma}_0^{\mathsf{res},n} = \mathbb{C}_0^{\mathsf{elD}}(D_0^n) : \boldsymbol{\varepsilon}_0^{\mathsf{res},n}$$

- reloading:

$\Delta\boldsymbol{\varepsilon}_0^{\mathsf{r}}$, D_0^{n+1}

$\downarrow$

Fibre	$\mathbb{C}_0^{\mathsf{SD}}(\kappa_0^{\mathsf{D}}, \mu_0^{\mathsf{SD}})$

$\downarrow$

$$\boldsymbol{\varepsilon}_0^{n+1} = \boldsymbol{\varepsilon}_0^{\mathsf{res},n} + \Delta\boldsymbol{\varepsilon}_0^{\mathsf{r}}$$
$$\boldsymbol{\sigma}_0^{n+1} = \boldsymbol{\sigma}_0^{\mathsf{res},n} + \mathbb{C}_0^{\mathsf{SD}}(D_0^{n+1}) : \Delta\boldsymbol{\varepsilon}_0^{\mathsf{r}}$$

Nonlinear equation for the MFH problem: ($\mathbb{S}$ the so-called Eshelby tensor)

$$\mathbf{F}_{\mathsf{MFH}} = \mathbb{C}_0^{\mathsf{SD}} : \left[\Delta\boldsymbol{\varepsilon}_{\mathsf{I}}^{\mathsf{r}} - \frac{1}{v_0} \mathbb{S}^{-1}(\mathsf{I}, \mathbb{C}_0^{\mathsf{SD}}) : (\Delta\boldsymbol{\varepsilon}_{\mathsf{I}}^{\mathsf{r}} - \Delta\boldsymbol{\varepsilon}^{\mathsf{r}}) \right] - \mathbb{C}_{\mathsf{I}}^{\mathsf{SD}} : \Delta\boldsymbol{\varepsilon}_{\mathsf{I}}^{\mathsf{r}}$$

NR iterative resolution: (i for fibre or matrix)

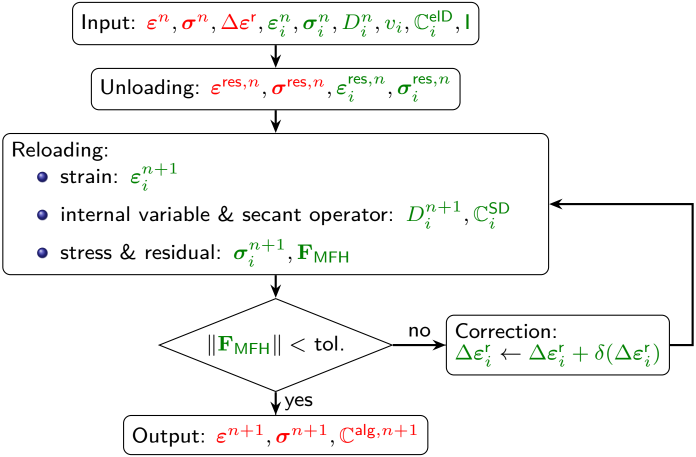

Appendix B.2 - Nonlinear analyses for 2-ply laminate-based node

Nonlinear equation to satisfy for the 2-ply laminate problem:

$$\mathbf{F}_{\mathsf{Lam}} = \begin{bmatrix} (\sigma_{\mathsf{A}}^{\mathsf{zz}} - \sigma_{\mathsf{B}}^{\mathsf{zz}}) + (\varepsilon_{\mathsf{A}}^{\mathsf{xx}} - \varepsilon_{\mathsf{Lam}}^{\mathsf{xx}}) \\ (\sigma_{\mathsf{A}}^{\mathsf{xz}} - \sigma_{\mathsf{B}}^{\mathsf{xz}}) + (\varepsilon_{\mathsf{A}}^{\mathsf{yy}} - \varepsilon_{\mathsf{Lam}}^{\mathsf{yy}}) \\ (\sigma_{\mathsf{A}}^{\mathsf{yz}} - \sigma_{\mathsf{B}}^{\mathsf{yz}}) + (\varepsilon_{\mathsf{A}}^{\mathsf{xy}} - \varepsilon_{\mathsf{Lam}}^{\mathsf{xy}}) \end{bmatrix} = \mathbf{0}$$

NR iterative resolution: (i for A-ply or B-ply)

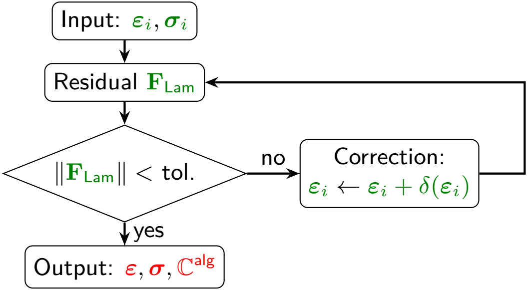

No nonlinear equation to be solved for the Voigt's mixtures problem

VM

Grain	$\boldsymbol{\theta}$	v	α
1 (matrix)	-	0.3544	-
2 (weft) & 3 (warp)	$[0/90, 89.99982, 0]$	0.0204	6.469
4 (weft) & 5 (warp)	$[0/90, 89.99986, 0]$	0.2737	151.095
6 (weft) & 7 (warp)	$[0/90, 89.99985, 0]$	0.0286	105.591

LVM

Grain	$\boldsymbol{\theta}$	v	α
1 (weft) & 2 (warp)	$[0/90, 82.432, 0]$	0.0314	216.645
3 (weft) & 4 (warp)	$[0/90, 90.648, 0]$	0.2618	258.721
5 (weft) & 6 (warp)	$[0/90, 90.651, 0]$	0.0770	195.969
7 (weft) & 8 (warp)	$[0/90, 93.161, 0]$	0.0241	181.194
9 (weft) & 10 (warp)	$[0/90, 116.875, 0]$	0.0176	21.032
11 (weft) & 12 (warp)	$[0/90, 92.995, 0]$	0.0179	247.153
13 (weft) & 14 (warp)	$[0/90, 80.612, 0]$	0.0105	204.540
15 (weft) & 16 (warp)	$[0/90, 102.166, 0]$	0.0073	123.377
17 (weft) & 18 (warp)	$[0/90, 88.039, 0]$	0.0312	298.981
19 (weft) & 20 (warp)	$[0/90, 66.960, 0]$	0.0211	23.852

VLM

Grain	$\boldsymbol{\theta}^{\mathrm{f}}$	$\boldsymbol{\theta}^{\mathrm{g}}$	v^{m}	v^{g}	α
1 (weft) & 2 (warp)	$[0, 89.963, 0]$	$[0/90, 0.479, 0]$	0.2291	0.2721	152.599
3 (weft) & 4 (warp)	$[0, 179.575, 0]$	$[0/90, -89.584, 0]$	0.5216	0.0204	542.078
5 (weft) & 6 (warp)	$[0, 89.698, 0]$	$[0/90, 8.230, 0]$	0.5514	0.0614	285.184
7 (weft) & 8 (warp)	$[0, 90.256, 0]$	$[0/90, -6.628, 0]$	0.5073	0.0681	207.968
9 (weft) & 10 (warp)	$[0, 90.108, 0]$	$[0/90, -2.391, 0]$	0.4424	0.0755	189.845
11 (weft) & 12 (warp)	$[0, 90.095, 0]$	$[0/90, -59.110, 0]$	0.9995	0.0024	367.619

Appendix D.1 - Uniaxial tensile test - Load-Unload

Comparison of the global responses:

	Strength [GPa]	CPU Time [mins]
DNS	831.481	1204
VM	848.241	0.05
rel. err. (%)	2.02	
VM-Mod.	882.647	
rel. err. (%)	6.15	
LVM	851.166	1
rel. err. (%)	2.37	
LVM-Mod.	870.576	
rel. err. (%)	4.70	
VLM	869.539	1
rel. err. (%)	4.58	

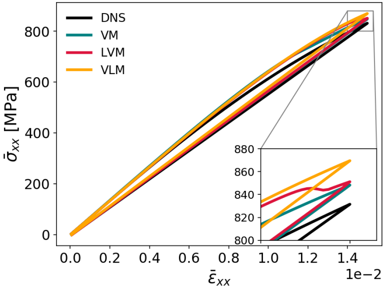

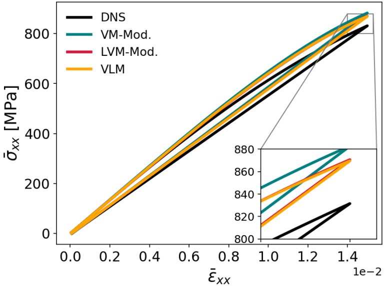

Comparison of the global responses: (predictions less accurate)

	Strength [GPa]	CPU Time [mins]
DNS	77.721	1435
VM	70.179	
rel. err. (%)	9.70	2
VM-Mod.	71.112	
rel. err. (%)	8.50	
LVM	69.838	
rel. err. (%)	10.14	37
LVM-Mod.	70.747	
rel. err. (%)	8.97	
VLM	69.155	9
rel. err. (%)	11.02	

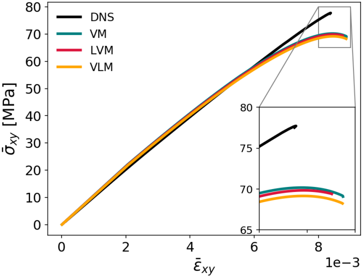

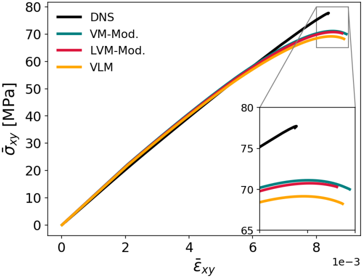

Comparison of the global responses: (predictions less accurate)

	Strength [GPa]	CPU Time [mins]
DNS	76.906	1149
VM	70.048	0.2
rel. err. (%)	8.92	
VM-Mod.	70.865	
rel. err. (%)	7.85	
LVM	69.677	4
rel. err. (%)	9.40	
LVM-Mod.	70.472	
rel. err. (%)	8.37	
VLM	69.004	2
rel. err. (%)	10.27